Article

Discovery Medicine 2024; 36(182): 546–558
https://doi.org/10.24976/Discov.Med.202436182.51

Unlocking the Therapeutic Potential of LncRNA *BLACAT1* in Hypopharynx Squamous Cell Carcinoma

Fan-li Liu[1,2,3,†], Zhan-cheng Zhang[1,4,†], Sheng-li Zhou[1,2], Xu-liang Liu[1,2], Wei Xu[1,2,*]

[1]Department of Otorhinolaryngology, Head and Neck Surgery, Shandong Provincial ENT Hospital, Cheeloo College of Medicine, Shandong University, 250012 Jinan, Shandong, China
[2]Shandong Provincial Key Laboratory of Otology, 250022 Jinan, Shandong, China
[3]Department of Otolaryngology Head & Neck Surgery, The Second Affiliated Hospital and Yuying Children's Hospital, Wenzhou Medical University, 325027 Wenzhou, Zhejiang, China
[4]Department of Otorhinolaryngology, The Fourth Hospital of Jinan, 250031 Jinan, Shandong, China
*Correspondence: xuwhns@126.com (Wei Xu)
[†]These authors contributed equally.
Published: 20 March 2024

Background: Identifying the key molecular targets in hypopharynx squamous cell carcinoma (HSCC) is crucial for understanding this prevalent and highly fatal type of head and neck tumor. The study aims to enhance comprehension of the HSCC process by accurately identifying these key molecular targets.

Materials and Methods: In this study, we examined 47 clinical tissue samples from individuals diagnosed with HSCC using RNA-seq high-throughput assay. Quantitative real-time PCR (RT-PCR) was used to compare long non-coding RNA (lncRNA) bladder cancer-associated transcript 1 (*BLACAT1*) expression in HSCC tissues versus adjacent non-tumor tissues. The influence of highly expressed lncRNA *BLACAT1* on prognostic survival was assessed. Subsequently, we cultured human pharynx squamous cell carcinoma FaDu cells. After reducing lncRNA *BLACAT1* expression, we assessed FaDu cell proliferation, invasion, and migration using Cell Counting kit-8 (CCK-8) assay, colony formation assay, EUD assay, Transwell assay, and scratch assay. Additionally, liquid chromatography-tandem mass spectrometry/mass spectrometry (LC-MS/MS) and western blotting analysis were used to analyze proteins that bind to lncRNA *BLACAT1*. During *in vivo* experiments, mice received subcutaneous injections of FaDu cells transfected with lncRNA *BLACAT1* shRNA or Scr plasmid (Control) in the dorsal region to observe and compare tumor growth. Lastly, tumor tissues underwent hematoxylin-eosin (HE) and immunohistochemical (IHC) staining.

Results: lncRNA *BLACAT1* was screened as one of the most significant genes among the group of differentially expressed lncRNAs. RT-PCR exhibited elevated lncRNA *BLACAT1* expression in HSCC tissues when compared to non-tumor tissues ($p < 0.001$). Furthermore, increased lncRNA *BLACAT1* expression correlated with advanced clinical stages, heightened lymphatic invasion, and a poor prognosis. Subsequent *in vitro* experiments solidified our observations, demonstrating lncRNA *BLACAT1*'s promotion of HSCC cell proliferation ($p < 0.05$), migration ($p < 0.01$), and invasion ($p < 0.01$) compared with the control group. Moreover, LC-MS/MS identified signal transducer and activator of transcription 3 (STAT3) and Prohibitin 2 (PHB2) as lncRNA *BLACAT1*-binding proteins and sh-lncRNA *BLACAT1* inhibits STAT3/AKT phosphorylation ($p < 0.01$) and alters the subcellular distribution of PHB2 and P21 compared with the control group ($p < 0.01$). Moreover, *in vivo* experiments showed that lncRNA *BLACAT1* inhibition suppresses tumorigenicity in an HSCC xenograft model compared to the control group ($p < 0.01$).

Conclusions: lncRNA *BLACAT1* is highly expressed in HSCC tumor tissues and plays a crucial role in the development of HSCC *in vitro* and *in vivo*. This increased expression may be caused by STAT3/AKT pathway activation, consequently inhibiting P21 expression through PHB2.

Keywords: long non-coding RNA Bladder cancer-associated transcript 1; hypopharynx squamous cell carcinoma; bioinformatics analysis; STAT3/AKT; PHB2/P21

Background

Hypopharynx squamous cell carcinoma (HSCC) represents about 3% of all cases of head and neck squamous cell carcinoma (HNSCC) [1]. Clinical detection of HSCC is often delayed due to its atypical symptoms and insidious onset, resulting in advanced-stage tumors. Therefore, the prognosis for patients with this condition is generally unfavorable [2,3]. The current treatment options for HSCC include surgery, radiotherapy, chemotherapy, and emerging immunotherapies. Despite some improvement in the survival rates of HSCC over the past three decades, the 5-year survival rate for advanced-stage hypopharyngeal cancer (T3 to T4) remains between 20% and 40% [4]. Thus, there is a pressing need to identify a new molecular biomarker

Copyright: © 2024 The Author(s). Published by Discovery Medicine. This is an open access article under the CC BY 4.0 license.
Note: *Discovery Medicine* stays neutral with regard to jurisdictional claims in published maps and institutional affiliations.

capable of predicting survival, detecting potential intervention targets, and assessing the effectiveness of therapeutic agents.

Long non-coding RNAs (lncRNAs), which are RNAs with minimal coding potential that exceed 200 nucleotides, have surfaced as a promising biomarker for diagnosing and predicting cancer [5,6]. LncRNA bladder cancer-associated transcript 1 (*BLACAT1*) was initially identified on the chromosome 1q32.1 locus in the patients with bladder cancer [7]. Previous studies have demonstrated that lncRNA *BLACAT1* is abundantly expressed in other cancer types, including pancreatic cancer [8], prostate cancer [9], and ovarian cancer [10]. Sun's study [11] demonstrated that *BLACAT1* could induce lung cancer progression through the activation of Sonic Hedgehog pathway signaling. Additionally, Chen *et al.* [12] associated *BLACAT1* with small-cell lung cancer's malignant status and prognosis while Liu *et al.* [13] reported upregulated *BLACAT1* in glioma, contributing to disease progression and predicting poor prognosis. However, the role of lncRNA *BLACAT1* in HSCC remains insufficiently acknowledged and extensively analyzed. Nevertheless, to our knowledge, there have been no reports addressing the diagnostic or prognostic significance of lncRNA *BLACAT1* in HSCC.

Therefore, this study investigated the gene expression patterns of lncRNA *BLACAT1* and its roles in HSCC tissues. Our findings indicate a strong association between elevated lncRNA *BLACAT1* expression levels and unfavorable HSCC survival outcomes. This correlation suggests the potential of lncRNA *BLACAT1* as a valuable prognostic marker for this disease. These results highlight the significance of lncRNA *BLACAT1* in HSCC by offering insights into its potential for diagnosis, prognosis, and targeted therapeutic interventions.

Materials and Methods

Clinical Sample Collection

From 2010 and 2015, we collected 47 sets of HSCC tissue samples and their corresponding adjacent noncancerous tissues from the Department of Otolaryngology at Shandong Provincial ENT Hospital. The ethical approval for clinical experiments was obtained from the ethics committee of Shandong Provincial ENT Hospital (XYK20200802). All participants included in the study had not undergone any prior chemoradiotherapy or biotherapy and had provided written informed consent. Following surgical excision, the tissues were immediately frozen in liquid nitrogen.

LncRNA Expression Analysis

Initially, we screened transcripts using Cuffcompare's class code to identify potential lncRNAs, retaining those present in at least two samples. To identify lncRNAs, our focus was on transcripts that did not overlap with known genes in the same direction, with lengths exceeding 200 nucleotides and expressing at minimum levels (fragment per kilobase per million reads (FPKM) 0.5 for transcripts with multiple exons and FPKM 2 for transcripts with a single exon). To ensure quality, we utilized CPC (Version 0.9-r2, Beijing, China) and Pfam-scan to filter transcripts, excluding those predicted to have coding potential while preserving those lacking it. The final lncRNA candidates, selected for further investigation, were chosen based on their presence in both technologies. Cuffdiff (Version 2.1.1, SanDiego, CA, USA) was utilized to calculate the FPKM for lncRNAs, identifying transcripts or genes differentially expression (adjusted p-value of 0.05, q-value of 0.05) between the two sets of HSCC tissues in biological replicates.

Prognostic Survival Analysis

The survival rates of patients with varying lncRNA *BLACAT1* expression levels were compared using survival analysis. Patient samples were divided into high and low-expression groups based on the median lncRNA *BLACAT1* expression value. Patient prognosis and survival time were assessed using a Kaplan-Meier (KM) survival curve generated using the R survival package. The survival curve underwent a log-rank test, revealing a significant difference in survival between the two groups based on lncRNA expression (p-values < 0.05).

Cell Culture and Transfection

The human pharynx squamous cell carcinoma FaDu cell line (HTB-43) was purchased from the American Type Culture Collection (ATCC, Manassas, VA, USA) and authenticated by Short Tandem Repeat (STR). No mycoplasma contamination was found in the mycoplasma testing. FaDu cells were grown in DMEM (Gibco, Grand Island, NY, USA) supplemented with 10% FBS. Plasmid-based shRNA was synthesized by cloning DNA oligonucleotides into the pleno-GFP vector (Shanghai Genechem Co., Ltd., Shanghai, China). The shRNA targeting lncRNA *BLACAT1* had the following target sequences: sh-1: 5′-AGGCUGGUUUCUGCCCUCAUCCUUU-3′, sh-2: 5′-GCCCAGCUUCUAGUCCUCUCCUUAU-3′. A random scrambled (Scr, control group) sequence (5′-AAGAAACCATGCAAAGTAAGGTT-3′), unrelated to human gene sequences, was used as a negative control. FaDu cells were plated at 1×10^5/mL density on 6-well plates for 24 hours before being infected with sh-lncRNA *BLACAT1* or Scr for 16 hours at 37 °C.

RNA Extraction and Quantitative Real-Time PCR

Total RNA from tissues or cultured cells was extracted using TRIzol (Thermo Fisher Scientific, Inc., Waltham, MA, USA) following the manufacturer's instructions. The relative expressions of lncRNA *BLACAT1* were measured using SYBR Premix Ex Taq (Takara, Dalian, China) and GAPDH as an internal con-

trol. The primer sequences are as follows: *BLACAT1*: 5′-GGAAGCUACAGCAGAGAAUTT-3′ (Forward), 5′-AUUCUCUGCUGUAGCUUCCTT-3′ (Reverse); GAPDH: 5′-AAGGTGAAGGTCGGAGTCAA-3′ (Forward), 5′-AATGAAGGGGTCATTGATGG-3′ (Reverse). The findings were normalized to GAPDH expression and analyzed using the $2^{-\Delta\Delta Ct}$ technique [14]. The experiment was repeated three times.

Cell Viability Assay

The cell viability was assessed using the Beyotime, China, Cell Counting Kit-8 (CCK-8, cas#C0037, Beyotime, Shanghai, China) assay. FaDu cells were plated at a density of 4×10^3 per well in 96-well culture plates with 100 µL of medium. After seeding, cells were cultured at 37 °C for 24, 48, and 72 hours. Subsequently, 10 µL of CCK-8 solution was added to each well and incubated for 2 hours at 37 °C after the incubation periods. The optical density at 450 nm was measured to quantify cell viability. The experiment was repeated three times.

Colony Formation Assay

The colony formation test evaluated the effect of lncRNA *BLACAT1* silencing on FaDu cell colonies. Transfected FaDu cells were first removed with trypsin and suspended in DMEM with 10% FBS. These cells were then placed in triplicate in 6-well plates, with 800 cells per well. Fresh growth media was used every three days. After 14 days of culture, the cellular colonies were rinsed with phosphate-buffered saline (PBS), fixed with 4% paraformaldehyde for 30–60 minutes, and subsequently stained with Giemsa (ECM550, Chemicon, Temecula, CA, USA) for 20 minutes. Only 50-cell colonies were manually counted under a light microscope. The experiment was repeated three times.

5-Ethynyl-2′-Deoxyuridine Labeling Assay

The 5-Ethynyl-2′-deoxyuridine imaging (EDU) kit (keyFluor647, cas#KGA330-50, Nanjing KeyGen Biotech Co., Ltd., Nanjing, China) was used to assess *in vitro* cellular proliferation following the manufacturer guidelines. EDU (EDU^+) was identified in three randomly selected sectors for each sample using a fluorescence microscope (Leica Microsystems GmbH, Wetzlar, Germany) and the percentage of cells incorporating EDU was subsequently calculated. The experiment was repeated three times.

Transwell Assays

The transwell assay assessed both cell migration and invasion. In this experiment, transfected FaDu cells (1×10^5/mL) were cultured in serum-free media in the top chamber while the bottom compartment was introduced with 500 µL of DMEM with 10% FBS. After 24 hours, migrated FaDu cells in the bottom compartment were fixed with 4% formaldehyde at room temperature for 15 minutes and stained with 0.1% crystal violet for 25 minutes. An inverted microscope was used to manually count invading cells in five random fields from each sample. Cell invasion was measured using identical transwell chambers coated with Matrigel (BD Biosciences, San Jose, CA, USA), however, the incubation time was prolonged to 36 hours due to the barrier. The experiment was repeated three times.

Scratch Assay

Cells were plated into 6-well culture plates and maintained to at least 95% confluence. Scratches were formed in the center of the wells using a 200 µL pipette tip, followed by incubation in a serum-free medium for a further 48 hours. After scratch formation, each well was gently rinsed with PBS. Images were captured under a phase contrast microscope at 0, 24, and 48 hours. The remaining scratch area was calculated using ImageJ software (Version 1.8.0; Media Cybernetics, Silver Springs, MD, USA) and normalized according to the initial scratch area. The experiment was repeated three times.

Liquid Chromatography-Tandem Mass Spectrometry/Mass Spectrometry (LC-MS/MS)

After fixing the cells with glutaraldehyde, cell lysis and chromatin breakage were performed using sonic degradation. Subsequently, a biotin-labeled oligo probe was added to the lysates to hybridize with lncRNA, which was isolated and purified using streptavidin magnetic beads, known for their affinity to biotin. Finally, the lncRNA-bound protein and DNA fragments were removed via RNaseA for subsequent analysis. 5 µL of peptides from each sample were separated by the nano-UPLC liquid phase system, EASY-nLC1200, and detected using an online mass spectrometer (QExactive). Analysis was performed on a 100 µm ID × 15 cm reversed-phase column (Reprosil-Pur 120 C18-AQ, 1.9 µm, Dr. Math). Mobile phase A constituted a 0.1% formic acid acetonitrile aqueous solution (2% acetonitrile), while liquid B consisted of a 0.1% formic acid acetonitrile aqueous solution (80% acetonitrile). The column was equilibrated with 100% solution A. The sample was directly loaded onto the chromatographic column from the autosampler, followed by separation via the chromatographic column. The enzymatic hydrolysis products were separated by nano-UPLC and then analyzed by online mass spectrometry using a Q-Exactive mass spectrometer (Thermo Finnigan, Waltham, MA, USA). The experiment was repeated three times.

Western Blot

To perform cell lysis, the Radio-Immunoprecipitation Assay (RIAP) lysis buffer (cas#P0013K, Beyotime, Shanghai, China) was used and established complete cell lysis. The extraction of nuclear and cytoplasmic proteins was accomplished using the Nuclear and Cytoplasmic Protein Extraction Kit (cas#P0028, Beyotime, Shanghai, China),

according to the manufacturer's guidelines. Proteins (30 µg) were separated by 10% sodium dodecyl sulfate polyacrylamide gel electrophoresis (SDS-PAGE) and subsequently transferred onto polyvinylidene fluoride (PVDF) membranes. The membranes were then blocked using 3% bovine serum albumin (BSA) and incubated overnight with primary antibodies at 4 °C. β-actin or Lamin B1 served as internal controls. The primary antibodies include the following: Lamin B1 Polyclonal antibody: sc-377000, Proteintch, 1:1000; β-Actin, TA-09, Biolabs, 1:2500; phosphorylated-AKT (P-AKT, Ser473) (D9E) XP® Rabbit mAb #4060, CST, 1:1000; AKT (pan) (40D4) Mouse mAb #2920, CST, 1:1000; phosphorylated-signal transducer and activator of transcription 3 (P-STAT3, Tyr705) (D3A7) XP® Rabbit mAb #9145, CST, 1:1000; STAT3 (124H6) Mouse mAb #9139, CST, 1:1000; Prohibitin 2 (PHB2) (E1Z5A) Rabbit mAb #14085, CST, 1:1000; p21 Waf1/Cip1 (12D1) Rabbit mAb #2947, CST, 1:1000. The following day, the membranes were incubated for 2 hours with corresponding secondary antibodies (Proteintch, Rosemont, IL, USA). Then, the goal proteins were detected using the Enhanced Chemiluminescent (ECL) kit (WBKLS0500, Millipore, Billerica, MA, USA) and quantified using Image J software (Version 1.8.0; Media Cybernetics, Silver Springs, MD, USA). The experiment was repeated three times.

Animals

Four-week-old male BALB/C nude mice were randomly assigned to the Scr and *BLACAT1*-sh groups (n = 5). These mice were subcutaneously injected in the dorsal region with FaDu cells (5×10^6) transfected with either lncRNA *BLACAT1* shRNA or Scr plasmid. Tumor volume was assessed every three days using digital calipers and calculated using the formula Volume = long diameter $\times$ short diameter^2 / 2. After inoculation, mice were humanely euthanized by carbon dioxide asphyxiation at 20% of chamber capacity per minute on day 28. After collecting the tumor tissues, these tissues were preserved using 4% paraformaldehyde for future study. This animal experiment was approved by the ethics committee of Shandong University (XYK-20200803).

Hematoxylin-Eosin (HE) and Immunohistochemical (IHC) Staining

The paraffin-embedded mouse tumor tissues were cut into 2 µm slices and stained with HE for histological examination. Following deparaffinization and rehydration, OriGene Technologies, Inc.'s target retrieval solution was employed according to the manufacturer's instructions to retrieve tissue antigens. After 16 min in the microwave, the slides were incubated with H_2O_2 to prevent endogenous peroxide for IHC staining. The slides were subsequently incubated overnight at 4 °C with Ki67-targeting primary antibodies (1:200; ZA-0502; OriGene Technologies, Inc., Rockwell, MD, USA). A secondary biotinylated goat anti-rabbit IgG antibody (1:500, SP-9001; OriGene Technologies, Inc., Rockwell, MD, USA) was incubated on the slides for 15 minutes. The positive Ki-67 expression rates in the tumor tissues were measured using an Olympus orthostatic microscope.

Statistical Analysis

Statistical analyses were performed using SPSS (Version 19.0, IBM, Armonk, NY, USA) and GraphPad Prism 8.0 (Dotmatics, Boston, MA, USA). Each experiment was repeated in triplicate and the mean value was taken as the final result. Normally distributed continuous data were presented as mean $\pm$ standard deviation (SD) and Student's *t*-tests were employed to compare two independent groups. For continuous data not conforming to a normal distribution, values were represented as the median [inter-quartile range] and compared using the Wilkinson signed-rank test. The relationship between the lncRNA *BLACAT1* expression and clinical prognostic indicators was assessed using the Chi-squared test, supplemented by Fisher's exact test when applicable. Survival curves for patients with different *BLACAT1* expression levels were established using the Kaplan-Meier method, and differences were compared using the log-rank test. The presented data represent the mean $\pm$ standard deviation. Statistical significance was defined as $p < 0.05$.

Results

Screening of Differentially Expressed LncRNAs in HSCC Tumor Tissues

Based on the established screening threshold, a total of 932 lncRNA genes exhibited significantly distinct expression profiles. Among these genes, 568 exhibited upregulation, while 364 displayed downregulation (Fig. 1A,B, respectively). Among the differentially expressed lncRNAs, lncRNA *BLACAT1* was notably higher in tumor tissues when compared to non-tumor tissues and demonstrated a noteworthy expression level (Log_2 FC = 2.07). Therefore, lncRNA *BLACAT1* was consequently selected for further evaluation. Notably, the biological processes associated with these lncRNAs primarily involve the cell cycle and cell proliferation (Fig. 1C,D).

The Relationship between the Expression Level of LncRNA BLACAT1 and Clinical Prognostic Indicators

To assess the expression level of lncRNA *BLACAT1* in HSCC tumor tissues, 47 pairs of such tissues along with their adjacent noncancerous tissues were subjected to RT-PCR analysis. The results revealed that the relative lncRNA *BLACAT1* expression levels in HSCC tissues were considerably higher than those found in their corresponding non-tumor tissues ($p < 0.001$ by Wilkinson signed rank test)

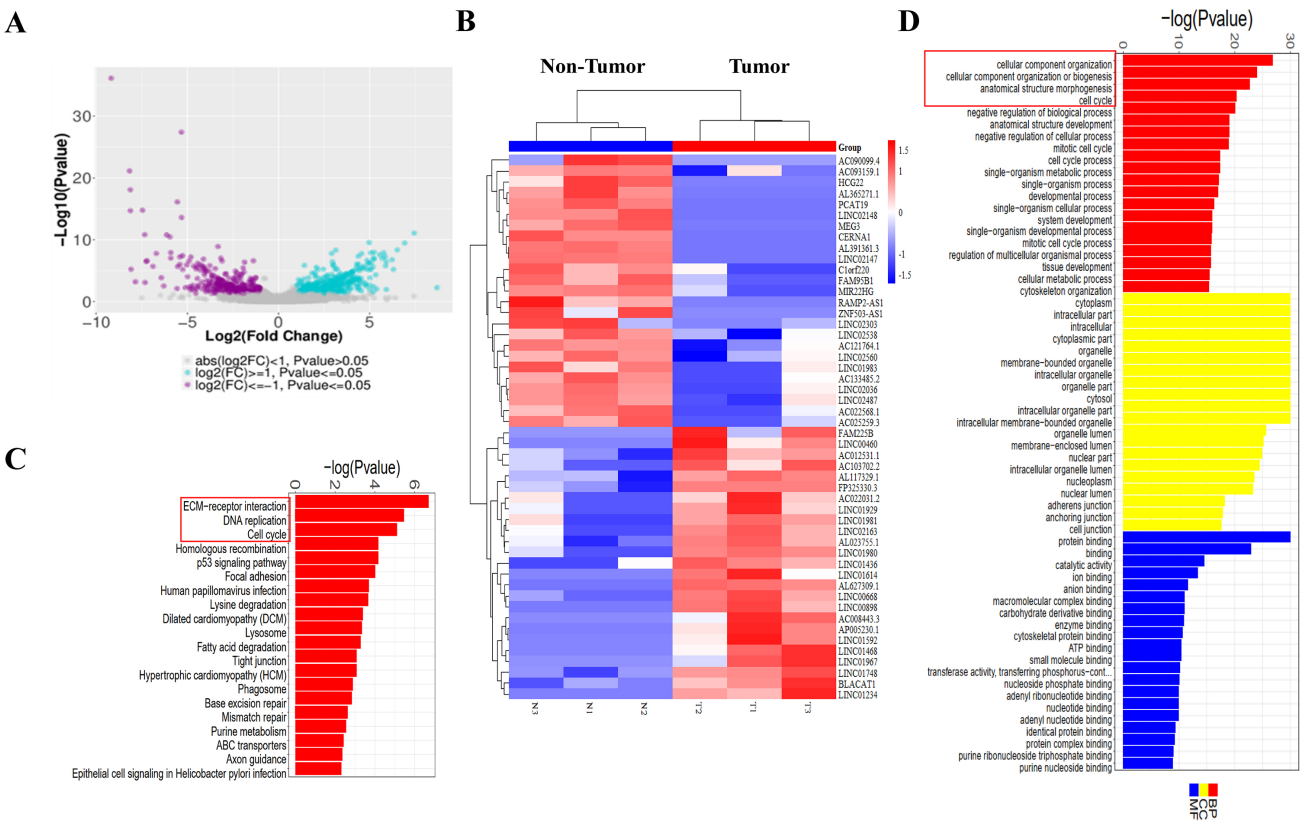

Fig. 1. Expression patterns of long non-coding RNAs (lncRNAs) in hypopharynx squamous cell carcinoma (HSCC) tissues. (A) The volcano plot displays differential expression of 932 lncRNAs, with 568 up-regulated and 364 down-regulated. (B) The heatmap of lncRNA transcript clustering highlights the significant enrichment of gene lncRNA bladder cancer-associated transcript 1 (*BLACAT1*) in tumor tissues compared to non-tumor tissues. (C,D) Kyoto Encyclopedia of Genes and Genomes (KEGG) and Gene Onotology (GO) databases predict the primary signal biological processes and pathways associated with the top candidate target lncRNAs.

(Fig. 2A), thus indicating a potential role of lncRNA *BLACAT1* in the pathogenesis of HSCC. To further investigate the connection between lncRNA *BLACAT1* expression and the patient characteristics, patients were stratified into two groups based on the median level of lncRNA *BLACAT1* expression (PCR expression: 4.20): high and low expression. The analysis of overall survival indicated that patients with higher lncRNA *BLACAT1* expression had a lower overall survival rate and a more unfavorable prognosis compared to those with lower lncRNA *BLACAT1* expression (Fig. 2B). Additionally, patients with higher lncRNA *BLACAT1* expression levels exhibited a higher incidence of lymph node metastasis and advance stage tumor ($p < 0.01$ by Chi-squared test) (Fig. 2C,D). Consequently, these data suggest a significant association between lncRNA *BLACAT1* and certain prognostic indicators in HSCC.

Inhibition of LncRNA BLACAT1 Suppresses FaDu Cell Proliferation

To investigate the biological function of lncRNA *BLACAT1* in FaDu cells, a series of loss-function experiments were conducted *in vitro*. qRT-PCR analysis revealed a significant reduction in lncRNA *BLACAT1* expression in FaDu cells after transfection with *BLACAT1*-sh1 and *BLACAT1*-sh2 ($p < 0.01$), confirming successful knockdown of lncRNA *BLACAT1* expression (Fig. 3A). Subsequent analysis of the CCK-8 assay indicated a notable decrease in cell proliferation upon lncRNA *BLACAT1* suppression ($p < 0.05$) (Fig. 3B). Furthermore, the colony formation assay demonstrated that FaDu cells lacking lncRNA *BLACAT1* exhibited significantly fewer colonies compared to cells transfected with the scramble sequence following a 14-day incubation ($p < 0.01$), indicating the involvement of lncRNA *BLACAT1* in promoting FaDu cell proliferation (Fig. 3C). Moreover, the impact of lncRNA *BLACAT1* on FaDu cell proliferation was also evaluated by EDU assay, establishing that the knockdown of lncRNA *BLACAT1* (both sh-1 and sh-2) led to a marked decrease in viable FaDu cells compared to the control group ($p < 0.01$) (Fig. 3D). Collectively, these findings suggest that lncRNA *BLACAT1* inhibition hinders FaDu cell proliferation.

Inhibition of LncRNA BLACAT1 Suppresses FaDu Cell Invasion and Migration

In response to the strong correlation observed between lncRNA *BLACAT1* and lymphoid metastasis in HSCC, our

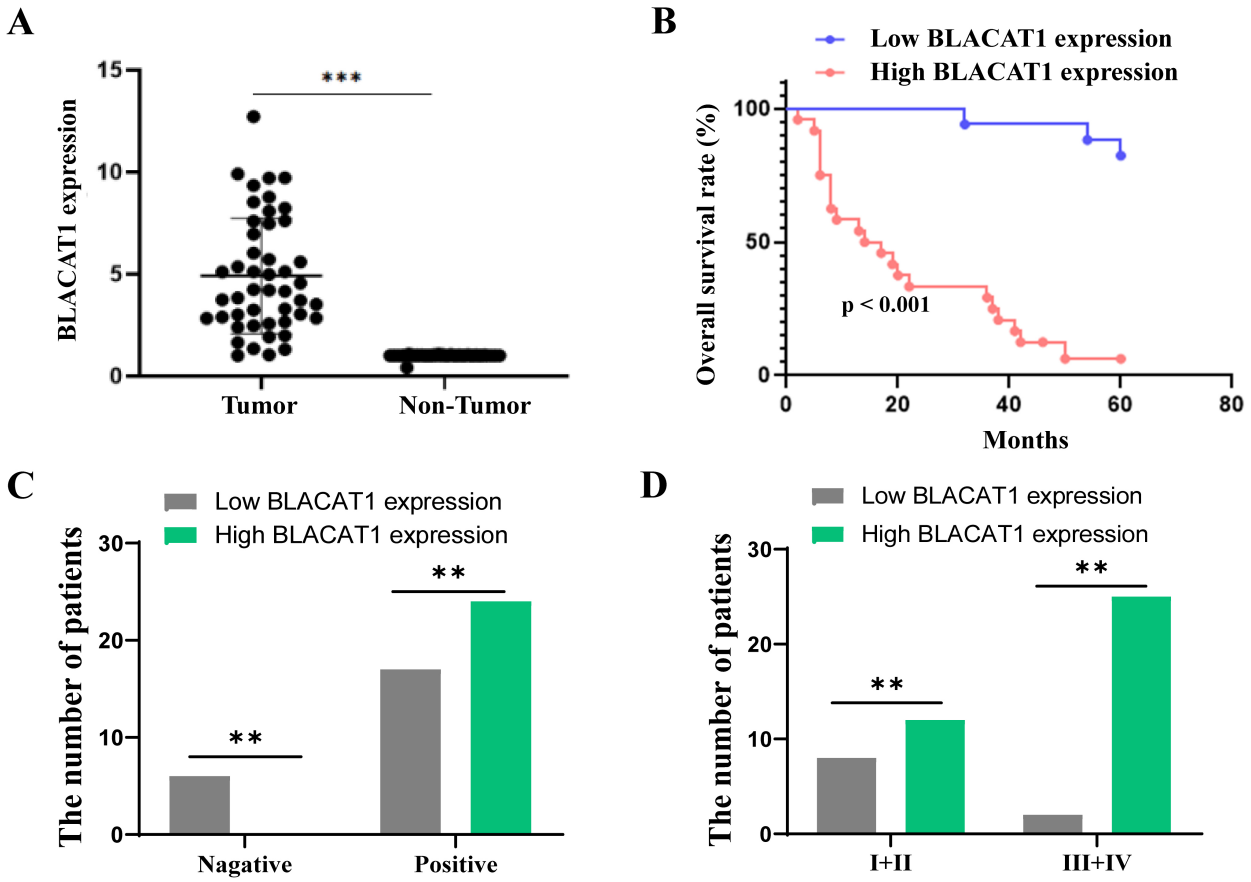

Fig. 2. Comparison of lncRNA *BLACAT1* expression levels in HSCC tissues and non-tumor tissues, and its relationship with clinicopathological characteristics. (A) The relative expression of lncRNA *BLACAT1* in HSCC tissues and non-tumor tissues was assessed using RT-PCR (n = 47, ***$p < 0.001$). (B) Kaplan-Meier (KM) analysis demonstrated a comparison of overall survival between high and low lncRNA *BLACAT1* expression. (C) The number of patients with lymph node metastasis, positive indicates having lymph node metastasis, negative indicates without lymph node metastasis (**$p < 0.01$). (D) The number of patients in different T classifications (**$p < 0.01$).

team conducted further investigations to assess the impact of lncRNA *BLACAT1* on cell invasion and migration using transwell assays. The outcomes of these experiments clearly indicated that suppression of lncRNA *BLACAT1* in FaDu cells significantly decreased the cells' invasive and migratory capabilities ($p < 0.01$) (Fig. 4A–C). This data implicates lncRNA *BLACAT1* in promoting the invasion and migration processes of hypopharyngeal carcinoma cells, implying that lncRNA *BLACAT1* could be identified as a pro-metastatic factor in these cells.

Inhibition of LncRNA BLACAT1 Suppresses the STAT3/AKT Signaling Pathway and Prevents PHB2 from Entering the Nucleus to Inhibit P21

To investigate how lncRNA *BLACAT1* regulates HSCC tumors, LC-MS/MS was performed to identify lncRNA *BLACAT1*-binding proteins, revealing signal transducer and activator of transcription 3 (STAT3) and PHB2 as lncRNA *BLACAT1*-binding proteins (Table 1). Additionally, our findings reveal that *BLACAT1*-sh did not alter the levels of STAT3 and AKT proteins compared to the control group. However, there was a significant reduction in the levels of P-STAT3 and P-AKT ($p < 0.01$) (Fig. 5A,B), indicating that lncRNA *BLACAT1* can activate the STAT3/AKT signaling pathway. Furthermore, the knockdown of lncRNA *BLACAT1* resulted in increased levels of both PHB2 and P21 proteins ($p < 0.01$) (Fig. 5C,D).

Given that PHB2 can act as a transcription factor by entering the nucleus [15], we conducted a nuclear and cytoplasmic protein separation experiment. The results demonstrated that in the control group, PHB2 was predominantly located in the nucleus, while P21 was primarily cytoplasmic. However, after sh-lncRNA *BLACAT1* treatment, there was an increase in cytoplasmic PHB2 and a decrease in nuclear PHB2. Additionally, P21 levels increased in the nucleus and further increased in the cytoplasm ($p < 0.01$) (Fig. 5E–G). These findings suggest that lncRNA *BLACAT1* may facilitate the nuclear entry of PHB2, which in turn may negatively regulate P21 as a transcription factor.

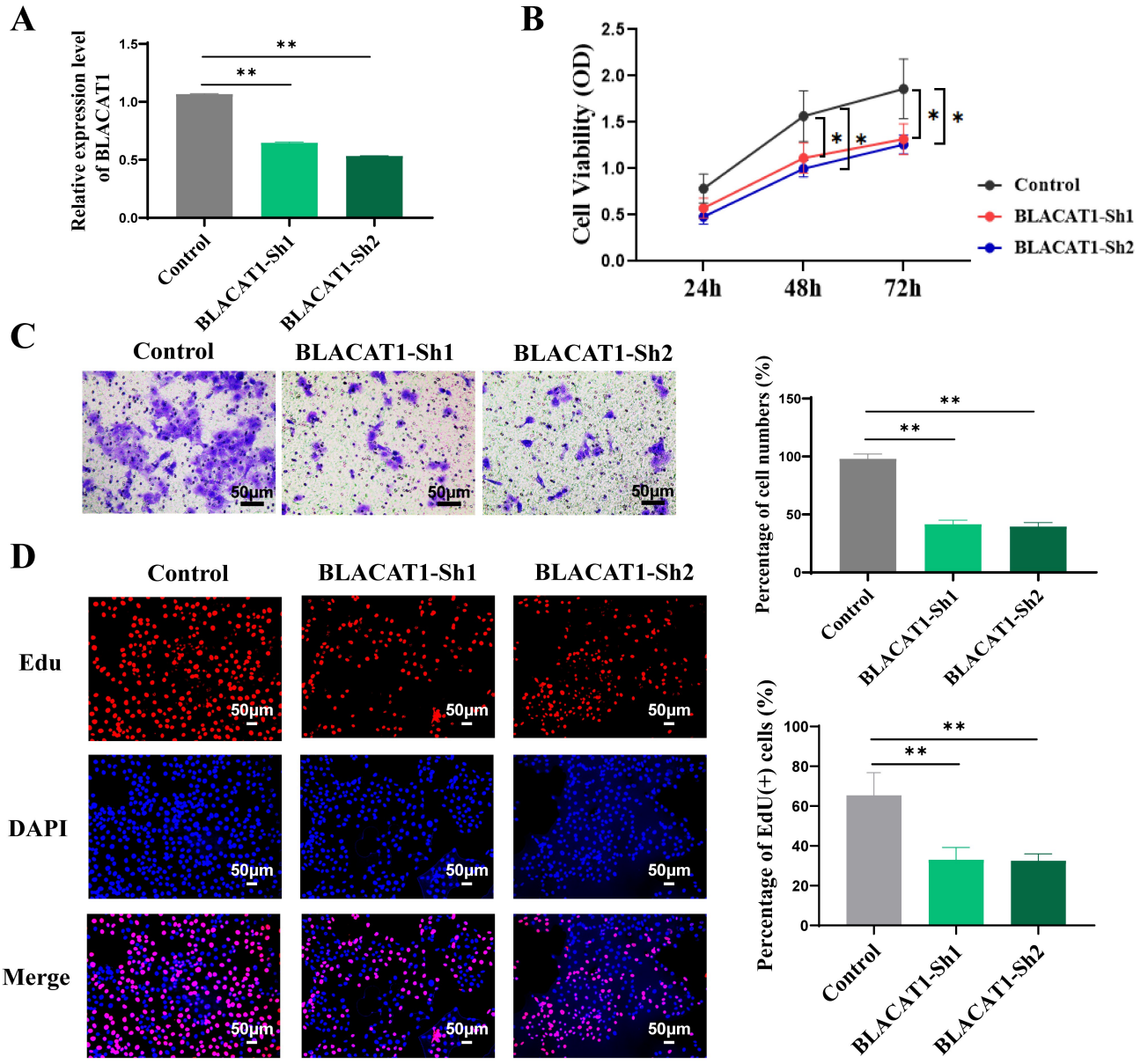

Fig. 3. Inhibition of lncRNA *BLACAT1* inhibited the proliferation of FaDu cells. (A) The expression of lncRNA *BLACAT1* in FaDu cells was assessed using the qRT-PCR. (B) FaDu cell viability was assessed using the Cell Counting kit-8 (CCK-8) assay. (C) Representative images and quantitative analysis of colony formation in FaDu cells. (D) Representative images and quantitative analysis of 5-Ethynyl-2′-deoxyuridine imaging (EDU) assay in FaDu cells. *$p < 0.05$, **$p < 0.01$, vs. control group (mean ± standard deviation (SD), n = 5).

Inhibition of LncRNA BLACAT1 Suppresses Tumorigenicity in a Xenograft Model of HSCC

To establish an animal model for xenograft investigation, we injected FaDu cells transfected with sh-lncRNA *BLACAT1* and controlled FaDu cells underneath the dorsal skin of nude mice. The primary objective of this model was to investigate the *in vivo* role of *BLACAT1*. We monitored tumor growth every three days and collected tumor samples on day 28. The lncRNA *BLACAT1*-sh group exhibited a significant reduction in tumor volumes and weight compared to the control group (Fig. 6A), thereby indicating that inhibiting lncRNA *BLACAT1* suppressed tumor growth ($p < 0.01$). Moreover, HE staining demonstrated increased necrosis within the tumor tissues due to *BLACAT1* inhibition, and immunohistochemical analysis revealed a decreased Ki-67 positive expression rate in the tumor tissues from mice injected with sh-lncRNA *BLACAT1* ($p < 0.01$) (Fig. 6B). Ultimately, we conclude that the downregulation of lncRNA *BLACAT1* hinders tumor growth and cell proliferation within the tumor tissues.

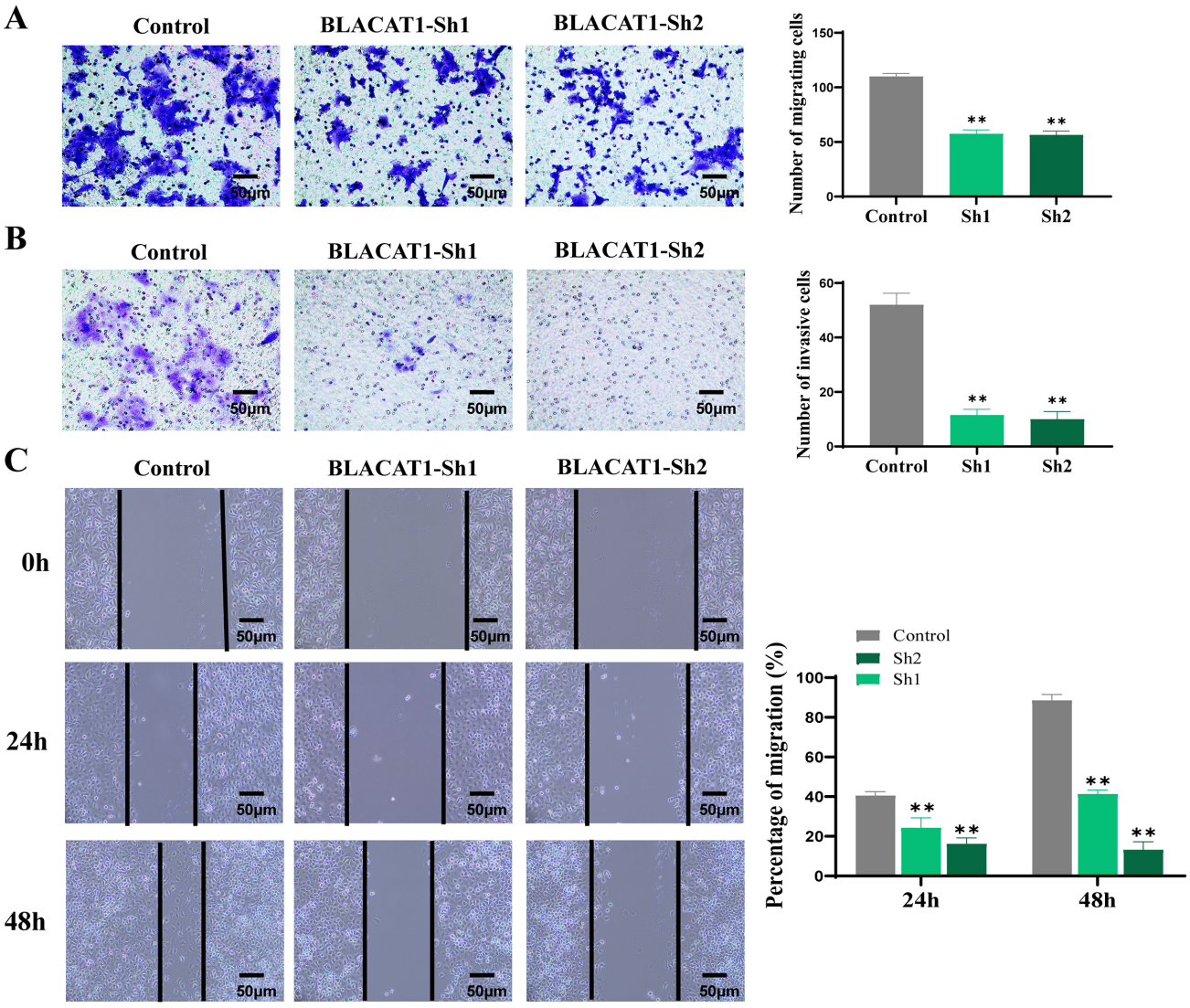

Fig. 4. Inhibition of lncRNA *BLACAT1* suppresses migration and invasion of FaDu cells. (A) Transwell assay was conducted to assess the invasion of FaDu cells transfected with lncRNA *BLACAT1*-siRNA (sh-1 and sh-2) and the scrambled control. (B) Transwell assay was conducted to assess the migration of FaDu cells transfected with lncRNA *BLACAT1*-siRNA (sh-1 and sh-2) and the scrambled control. (C) The scratch assay demonstrated that inhibition of lncRNA *BLACAT1* suppresses FaDu cell migration. $^{**}p < 0.01$, vs. control group (mean ± SD, n = 5).

Discussion

Given the involvement of lncRNA in various cellular processes, its abnormal expression has been associated with several diseases and plays a vital role in the progression and development of tumors [16]. Previous research extensively investigated the role of lncRNA *BLACAT1* in tumor development and progression in different tumor tissues [17,18]. However, comprehensive data regarding the expression characteristics of lncRNA *BLACAT1* in HSCC remains limited. In this study, we analyzed RNA-seq data from clinical HSCC samples and found that the expression of lncRNA in HSCC tissues exhibited a higher number of abnormal gene expressions, including 568 up-regulated genes and 364 down-regulated genes compared to normal non-tumor tissues. Among the genes potentially associated with HSCC, lncRNA *BLACAT1* was selected to further analyze its expression levels. We confirmed through RT-PCR testing that lncRNA *BLACAT1* was up-regulated in HSCC tissues.

Recently, lncRNA *BLACAT1* was identified in several head and neck cancers, exhibiting multiple regulatory roles. Gou *et al.* [19] revealed that lncRNA *BLACAT1* expression exhibited higher levels in HNSCC tissues compared to normal tissues and that this increased expression correlated with a poorer prognosis in HNSCC patients, and knocking down lncRNA *BLACAT1* increased HNSCC cell apoptosis and significantly reduced radiotherapy-resistance [19]. In this study, we also observed that patients with higher lncRNA *BLACAT1* expression had a lower overall survival

Table 1. LncRNA *BLACAT1*-binding proteins identified by LC-MS/MS.

Proteins	Score	iBAQ	MS.MS.count.con	MS.MS.count.Lnc	MS.MS.count.U1
STAT3	19.499	144860	0	2	0
PHB2	49.235	2041700	0	7	0

Abbreviations: LC-MS/MS, liquid chromatography-tandem mass spectrometry/mass spectrometry; iBAQ, intensity-based absolute quantification; MS, mass spectrometry; STAT3, signal transducer and activator of transcription 3; PHB2, Prohibitin 2.

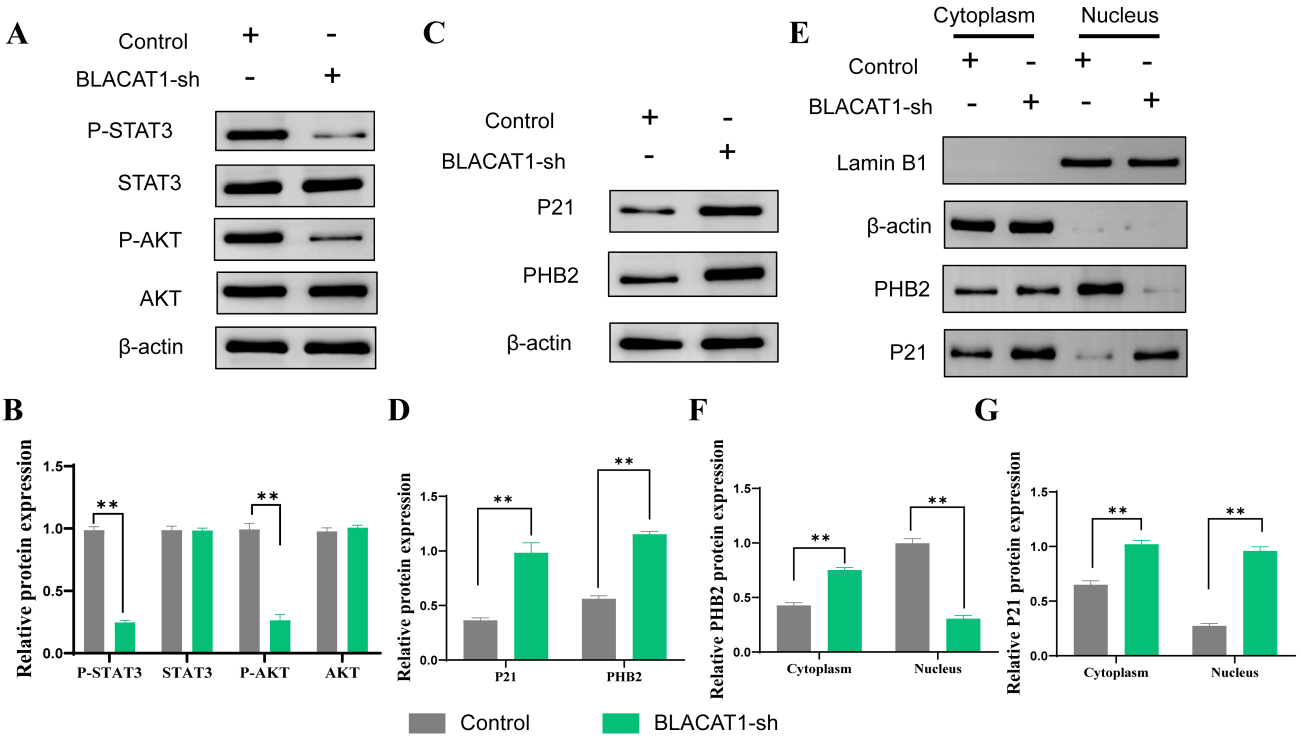

Fig. 5. LncRNA *BLACAT1* activates the STAT3/AKT signaling pathway and affects the distribution of PHB2 and P21 in FaDu cells. (A,B) Western blot was used to determine the expression of phosphorylated STAT3 (P-STAT3), STAT3, P-AKT, AKT, and β-actin in FaDu cells transfected with scrambled sequence (Scr) or lncRNA *BLACAT1*-sh1+sh2 (*BLACAT1*-sh). (C,D) Western blot was used to determine the expression of PHB2, P21, and β-actin in FaDu cells transfected with Scr or *BLACAT1*-sh. (E–G) After the separation of nuclear and cytoplasmic proteins, a western blot was used to determine the expression of Lamin B1, β-actin, PHB2, and P21 in FaDu cells transfected with Scr or *BLACAT1*-sh. $^{**}p < 0.01$ (mean $\pm$ SD, n = 3).

rate and a more unfavorable prognosis. Further *in vitro* and *in vivo* experiments showed that the inhibition of lncRNA *BLACAT1* suppresses proliferation, migration, and invasion of FaDu cells *in vitro* and suppresses tumorigenicity *in vivo*. These results collectively demonstrated that lncRNA *BLACAT1* plays a crucial role in the advancement of HSCC. The significance of lncRNA *BLACAT1* lies in its potential to contribute to the diagnosis, targeted treatment, and prognosis of individuals affected by HSCC.

STAT3 is an important member of the STAT family and is vital to the transduction of cellular signals and activation of transcription [20]. Additionally, STAT3 has the capability to promote tumor cell growth, proliferation, invasion, and metastasis through numerous pathways [21]. Activation of STAT3 primarily occurs via tyrosine residue phosphorylation. Recent studies suggest that the expression of P-STAT3 is significantly elevated in various cancers, and it is closely correlated with cancer cell proliferation, invasion, infiltration, clinical staging, and prognosis [22–25]. AKT, when overexpressed or phosphorylated, contributes to oncogenesis in multiple human cancers [26]. When the kinase phosphatidylinositol-3-kinase (PI3K) receives a foreign signal and is activated, it adds a phosphate group to PIP2 on the cell membrane, converting it to phosphatidylinositol 3 phosphate (PIP3). Subsequently, the second messenger PIP3 binds to AKT and activates it by phosphorylating it to p-AKT. The mechanistic target of rapamycin (mTOR) is a direct effector of AKT that can be phosphorylated by activated AKT, and activation of mTOR can cause phosphorylation of downstream STAT3 signaling molecules [27,28]. Recent investigations have revealed that AKT binds and phosphorylates salt-inducible kinase 1

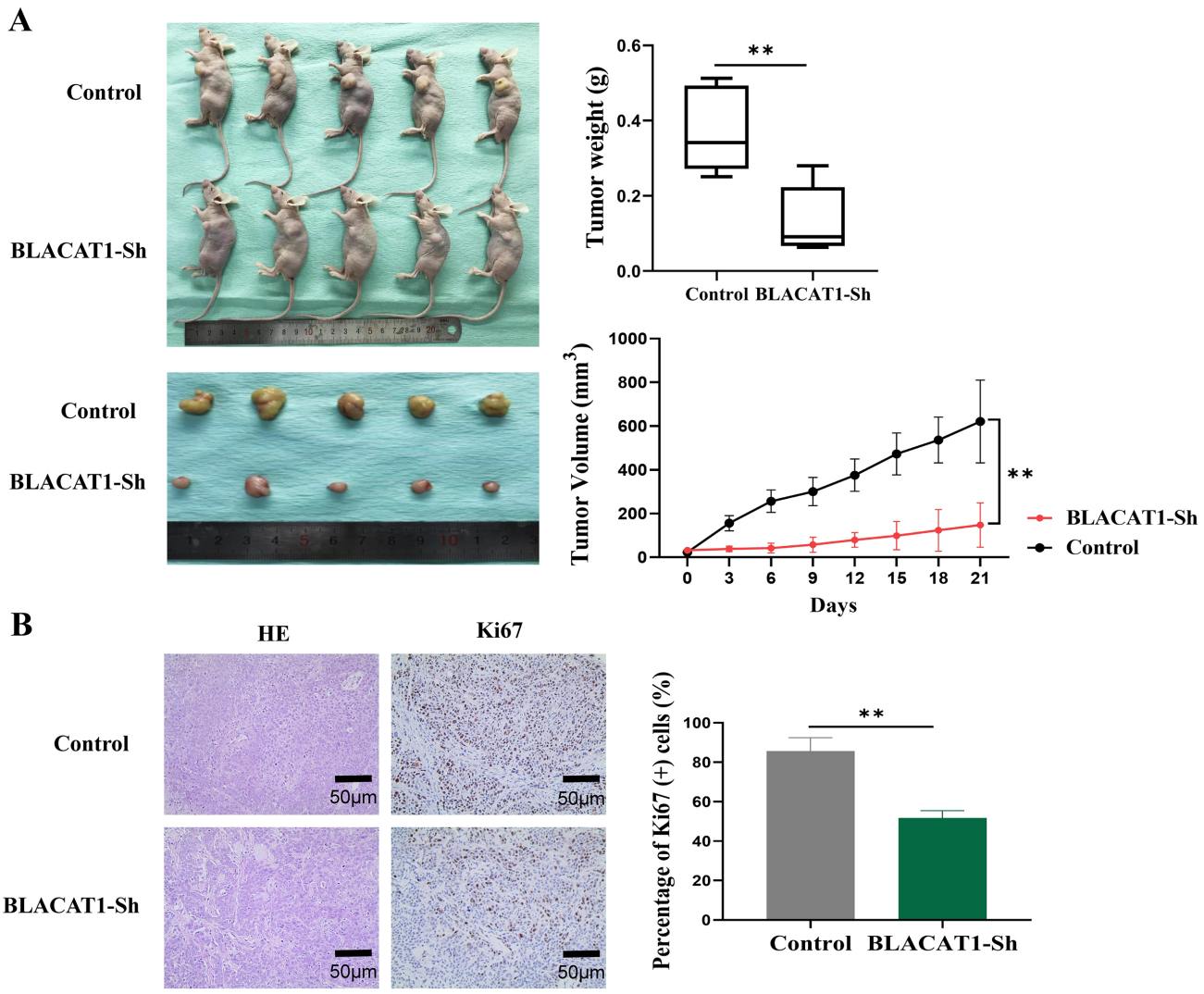

Fig. 6. Inhibition of lncRNA *BLACAT1* suppresses tumorigenicity in a xenograft model of HSCC. (A) Images of mice and tumors isolated from the sh-lncRNA *BLACAT1* (*BLACAT1*-sh) and control groups, and the tumor weight and volume of the two groups. (B) Hematoxylin-eosin (HE) staining of tumor tissues, and immunohistochemical detection of Ki67-positive cells in tumor samples from mice in the two groups. Statistical significance was determined using a *t*-test. ** $p < 0.01$ (mean ± SD, n = 5).

(SIK1), which opposes SIK1-mediated inhibition of STAT3 and fosters tumorigenesis [29]. Our investigation discovered that sh-lncRNA *BLACAT1* did not impact the protein levels of STAT3 and AKT in FaDu cells although it inhibited their phosphorylation. This finding is in line with prior studies suggesting elevated expression of lncRNA *BLACAT1* in HSCC, which triggers the STAT3/AKT signaling pathway and propels cancer progression.

PHB2 is a highly conserved protein belonging to the prohibitin family, pivotal in numerous cellular processes including transcription, nuclear signaling, cell division, and cell membrane metabolism [15]. The involvement of PHB2 in cancer remains controversial. In the case of most human cancers, such as prostate cancer and non-small cell lung cancer [30,31], tumor progression is facilitated by the overexpression of PHB2. However, in specific cancers like breast cancer and osteosarcoma [32,33], PHB2 impedes tumor progression. PHB2 function is dependent on its location within the cell. When found outside the nucleus, PHB2 participates in signaling and scaffolding, forming cyclic complexes alongside PHB1 to regulate processes, such as mitophagy, apoptosis, and cell proliferation. Conversely, when found inside the nucleus, PHB2 can act as a transcription factor or interact with other transcription factors [15]. Our study on nucleocytoplasmic isolation has displayed that the depletion of lncRNA *BLACAT1* results in an elevation of cytoplasmic PHB2 content and a reduction of nuclear PHB2 content. These findings suggest that lncRNA *BLACAT1* assists in the transportation of PHB2 to the nucleus to carry out its regulatory functions in HSCC.

Cancer is caused by an imbalance between cell proliferation and cell death. Numerous studies have proposed different mechanisms for carcinogenesis and identified novel anticancer treatments. P21, a recognized cyclin-dependent

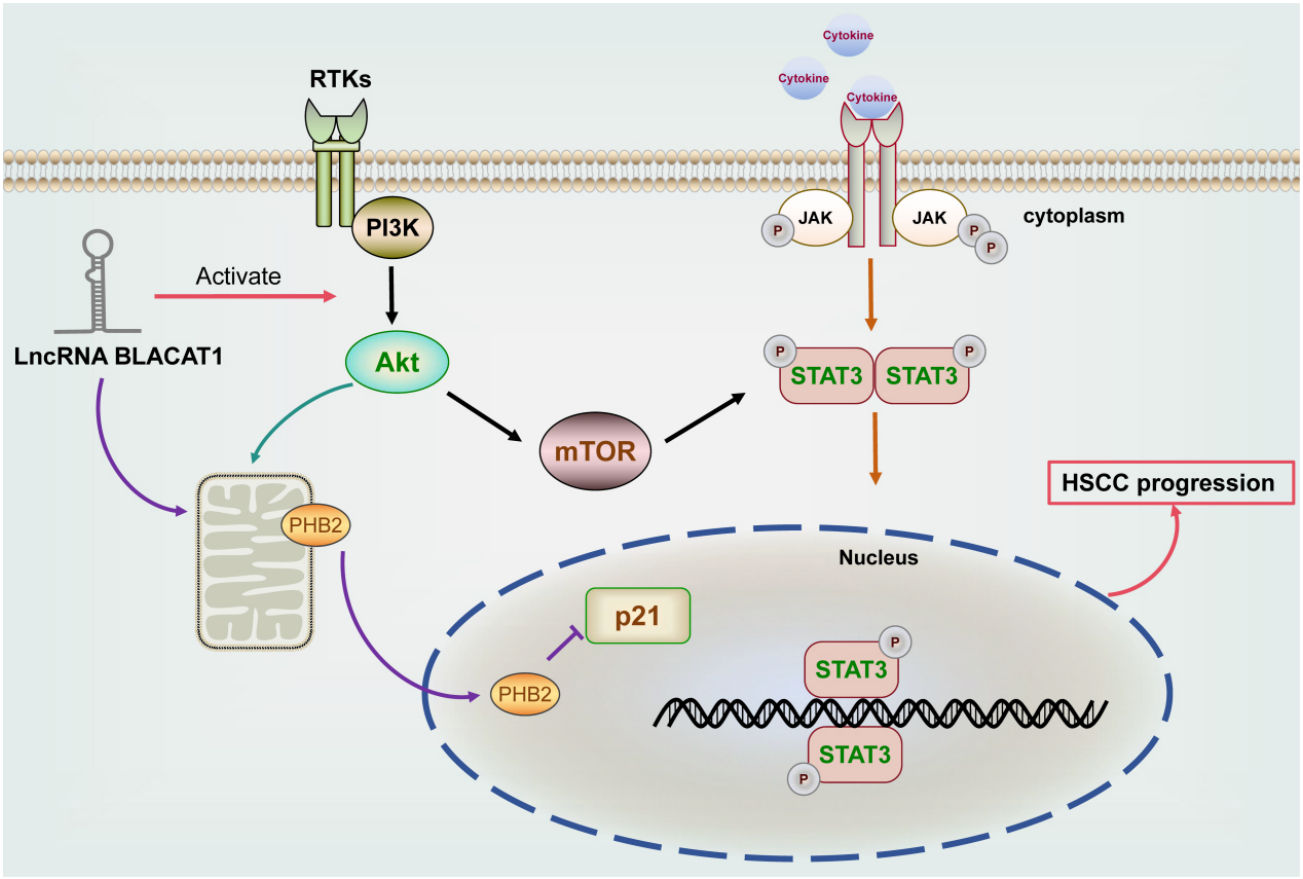

Fig. 7. The mechanism diagram that lncRNA *BLACAT1* regulates HSCC. The figure was created by scienceslides software (version 2016, VisiScience Corp., Chapel Hill, NC, USA)

kinase inhibitor, is regarded as a promising anticancer agent due to its dual role as a tumor suppressor and apoptosis inhibitor [34]. P21 has been identified as a potential target for cancer therapy. Our research indicates that *BLACAT1*-sh can effectively increase P21 expression, aligning with previous reports linking increased P21 levels to tumor growth inhibition. According to the findings of Keiko Taniguchi *et al.* [35], it was concluded that PHB2 can inhibit the transcriptional activity of P21. However, our experimental results seem to contradict this conclusion. Nevertheless, the nucleocytoplasmic separation results provide a plausible explanation for this inconsistency. Despite an overall PHB2 increase following lncRNA *BLACAT1* suppression, the rise specifically occurred in the cytoplasm. Mass spectrometry results also showed that lncRNA *BLACAT1* can bind to PHB2. Consequently, *BLACAT1*-sh led to the blockage or reduction of PHB2 entering the nucleus, thereby weakening its inhibitory effect on P21.

Some existing literature suggests crosstalk between PHB2 and AKT. In various diseases, PHB2 has been found to inhibit AKT activity and resultantly reduce cell migration, while also enhancing AKT to promote cell migration. Additionally, AKT can phosphorylate PHB2, thereby regulating nuclear mitochondrial activity and further promoting cell survival [11]. Moreover, P21 can regulate the AKT signaling pathway. For instance, P21 inhibition can activate AKT kinase to trigger ROS-induced autophagy and impact tumor growth rate [36], which is supported by the current study. We have discovered that lncRNA *BLACAT1* not only activates the STAT3/AKT signaling pathway but also regulates and promotes PHB2's nuclear entry, inhibits P21 activation, and promotes HSCC progression (Fig. 7). However, the extent of such crosstalk and the regulatory role of lncRNA *BLACAT1* in the translocation of PHB2 to the nucleus remains unclear. Our upcoming research will focus on investigating the potential crosstalk between the two pathways of lncRNA *BLACAT1* in HSCC and exploring the mechanisms by which lncRNA modulates the nuclear entry of PHB2.

Conclusions

High expression of lncRNA *BLACAT1* in HSCC patients correlated with lower survival rates and poor prognosis. Inhibition of lncRNA *BLACAT1* suppresses FaDu cell proliferation, migration, and invasion *in vitro* and suppresses tumorigenicity *in vivo*. Additionally, we have noted that lncRNA *BLACAT1* may drive cancer progression by triggering the STAT3/AKT and PHB2/P21 signaling path-

ways. Our study proposes that lncRNA *BLACAT1* might serve as a significant indicator for prognostic prediction in HSCC, thereby setting the groundwork for deeper mechanistic investigations.

Availability of Data and Materials

Data involved in the present work are available from the corresponding author upon request.

Author Contributions

FL, ZZ and WX designed the research study. FL, ZZ and WX performed the research. SZ and XL provided help and advice on experiments. SZ and XL analyzed the data. All authors contributed to editorial changes in the manuscript. All authors read and approved the final manuscript. All authors have participated sufficiently in the work and agreed to be accountable for all aspects of the work.

Ethics Approval and Consent to Participate

The study was conducted in accordance with the Declaration of Helsinki, and approved by the ethics committee of Shandong Provincial ENT Hospital (XYK20200802). Written informed consent has been obtained from the patients to publish this paper. The animal experiment was approved by the ethics committee of Shandong University (XYK-20200803).

Acknowledgment

Not applicable.

Funding

This research was funded by National Natural Science Foundation of China (82172961), the Major Science and Technology Plan Project of Hainan Province (ZDKJ202005).

Conflict of Interest

The authors declare no conflict of interest.

References

[1] Cooper JS, Porter K, Mallin K, Hoffman HT, Weber RS, Ang KK, *et al*. National Cancer Database report on cancer of the head and neck: 10-year update. Head & Neck. 2009; 31: 748–758.

[2] Newman JR, Connolly TM, Illing EA, Kilgore ML, Locher JL, Carroll WR. Survival trends in hypopharyngeal cancer: a population-based review. The Laryngoscope. 2015; 125: 624–629.

[3] Hall SF, Groome PA, Irish J, O'Sullivan B. The natural history of patients with squamous cell carcinoma of the hypopharynx. The Laryngoscope. 2008; 118: 1362–1371.

[4] Vengaloor Thomas T, Nittala MR, Bhanat E, Albert AA, Vijayakumar S. Management of Advanced-stage Hypopharyngeal Carcinoma: 25-Year Experience from a Tertiary Care Medical Center. Cureus. 2020; 12: e6679.

[5] Lu H, Liu H, Yang X, Ye T, Lv P, Wu X, *et al*. LncRNA BLACAT1 May Serve as a Prognostic Predictor in Cancer: Evidence from a Meta-Analysis. BioMed Research International. 2019; 2019: 1275491.

[6] Tan YT, Lin JF, Li T, Li JJ, Xu RH, Ju HQ. LncRNA-mediated posttranslational modifications and reprogramming of energy metabolism in cancer. Cancer Communications (London, England). 2021; 41: 109–120.

[7] He W, Cai Q, Sun F, Zhong G, Wang P, Liu H, *et al*. linc-UBC1 physically associates with polycomb repressive complex 2 (PRC2) and acts as a negative prognostic factor for lymph node metastasis and survival in bladder cancer. Biochimica et Biophysica Acta. 2013; 1832: 1528–1537.

[8] Zhou X, Gao W, Hua H, Ji Z. LncRNA-BLACAT1 Facilitates Proliferation, Migration and Aerobic Glycolysis of Pancreatic Cancer Cells by Repressing CDKN1C via EZH2-Induced H3K27me3. Frontiers in Oncology. 2020; 10: 539805.

[9] Liao B, Chen S, Li Y, Yang Z, Yang Y, Deng X, *et al*. LncRNA BLACAT1 Promotes Proliferation, Migration and Invasion of Prostate Cancer Cells via Regulating miR-29a-3p/DVL3 Axis. Technology in Cancer Research & Treatment. 2021; 20: 1533033820972342.

[10] Yang H, Qi Y, Wang XL, Gu JJ, Shi TM. Down-regulation of lncRNA BLACAT1 inhibits ovarian cancer progression by suppressing the Wnt/β-catenin signaling pathway via regulating miR-519d-3p. Molecular and Cellular Biochemistry. 2020; 467: 95–105.

[11] Sun J, Jia J, Yuan W, Liu S, Wang W, Ge L, *et al*. LncRNA BLACAT1 Accelerates Non-small Cell Lung Cancer Through Up-Regulating the Activation of Sonic Hedgehog Pathway. Frontiers in Oncology. 2021; 11: 625253.

[12] Chen W, Hang Y, Xu W, Wu J, Chen L, Chen J, *et al*. BLACAT1 predicts poor prognosis and serves as oncogenic lncRNA in small-cell lung cancer. Journal of Cellular Biochemistry. 2019; 120: 2540–2546.

[13] Liu N, Hu G, Wang H, Wang Y, Guo Z. LncRNA BLACAT1 regulates VASP expression via binding to miR-605-3p and promotes giloma development. Journal of Cellular Physiology. 2019; 234: 22144–22152.

[14] Livak KJ, Schmittgen TD. Analysis of relative gene expression data using real-time quantitative PCR and the 2(-Delta Delta C(T)) Method. Methods (San Diego, Calif.). 2001; 25: 402–408.

[15] Qi A, Lamont L, Liu E, Murray SD, Meng X, Yang S. Essential Protein PHB2 and Its Regulatory Mechanisms in Cancer. Cells. 2023; 12: 1211.

[16] Do H, Kim W. Roles of Oncogenic Long Non-coding RNAs in Cancer Development. Genomics & Informatics. 2018; 16: e18.

[17] Han W, Yu F, Guan W. Oncogenic roles of lncRNA BLACAT1 and its related mechanisms in human cancers. Biomedicine & Pharmacotherapy = Biomedecine & Pharmacotherapie. 2020; 130: 110632.

[18] Zhu M, Li X, Zhu S, Li P, Min L, Zhang S. Long non-coding RNA BLACAT1, a novel promising biomarker and regulator of human cancers. Biomedicine & Pharmacotherapy = Biomedecine & Pharmacotherapie. 2020; 132: 110808.

[19] Gou C, Han P, Li J, Gao L, Ji X, Dong F, *et al*. Knockdown of lncRNA BLACAT1 enhances radiosensitivity of head and neck squamous cell carcinoma cells by regulating PSEN1. The British Journal of Radiology. 2020; 93: 20190154.

[20] Shuai K, Stark GR, Kerr IM, Darnell JE, Jr. A single phosphotyrosine residue of Stat91 required for gene activation by interferon-gamma. Science (New York, N.Y.). 1993; 261: 1744–1746.

[21] Yang Y, Tang J, Cui C. Research progress on the mechanism of abnormally high activation of STAT3 to promote tumorigenesis and development. Chinese Journal of Immunology. 2017; 34: 1750–1754. (In Chinese)

[22] Shi S, Ma HY, Zhang ZG. Clinicopathological and prognostic value of STAT3/p-STAT3 in cervical cancer: A meta and bioinformatics analysis. Pathology, Research and Practice. 2021; 227: 153624.

[23] Ma RJ, Zheng QM, Zhang N, Sun ZG. Clinicopathological Significance of STAT3 and p-STAT3 among 91 Patients with Adenocarcinoma of the Esophagogastric Junction. Disease Markers. 2022; 2022: 9311684.

[24] Groot JD, Ott M, Wei J, Kassab C, Fang D, Najem H, *et al*. A first-in-human Phase I trial of the oral p-STAT3 inhibitor WP1066 in patients with recurrent malignant glioma. CNS Oncology. 2022; 11: CNS87.

[25] Wang Y, Wang Q, Tang CH, Chen HD, Hu GN, Shao JK, *et al*. p-STAT3 expression in breast cancer correlates negatively with tumor size and HER2 status. Medicine. 2021; 100: e25124.

[26] Revathidevi S, Munirajan AK. Akt in cancer: Mediator and more. Seminars in Cancer Biology. 2019; 59: 80–91.

[27] Wang J, Lv X, Guo X, Dong Y, Peng P, Huang F, *et al*. Feedback activation of STAT3 limits the response to PI3K/AKT/mTOR inhibitors in PTEN-deficient cancer cells. Oncogenesis. 2021; 10: 8.

[28] Liu Y, Deng S, Zhang Z, Gu Y, Xia S, Bao X, *et al*. 6-Gingerol attenuates microglia-mediated neuroinflammation and ischemic brain injuries through Akt-mTOR-STAT3 signaling pathway. European Journal of Pharmacology. 2020; 883: 173294.

[29] Sun Z, Jiang Q, Gao B, Zhang X, Bu L, Wang L, *et al*. AKT Blocks SIK1-Mediated Repression of STAT3 to Promote Breast Tumorigenesis. Cancer Research. 2023; 83: 1264–1279.

[30] Shen Y, Gao Y, Yuan H, Cao J, Jia B, Li M, *et al*. Prohibitin-2 negatively regulates AKT2 expression to promote prostate cancer cell migration. International Journal of Molecular Medicine. 2018; 41: 1147–1155.

[31] Wu B, Chang N, Xi H, Xiong J, Zhou Y, Wu Y, *et al*. PHB2 promotes tumorigenesis *via* RACK1 in non-small cell lung cancer. Theranostics. 2021; 11: 3150–3166.

[32] Yoshimaru T, Komatsu M, Matsuo T, Chen YA, Murakami Y, Mizuguchi K, *et al*. Targeting BIG3-PHB2 interaction to overcome tamoxifen resistance in breast cancer cells. Nature Communications. 2013; 4: 2443.

[33] Toki S, Yoshimaru T, Matsushita Y, Aihara H, Ono M, Tsuneyama K, *et al*. The survival and proliferation of osteosarcoma cells are dependent on the mitochondrial BIG3-PHB2 complex formation. Cancer Science. 2021; 112: 4208–4219.

[34] Parveen A, Akash MSH, Rehman K, Kyunn WW. Dual Role of p21 in the Progression of Cancer and Its Treatment. Critical Reviews in Eukaryotic Gene Expression. 2016; 26: 49–62.

[35] Taniguchi K, Matsumura K, Kageyama S, Ii H, Ashihara E, Chano T, *et al*. Prohibitin-2 is a novel regulator of $p21^{WAF1/CIP1}$ induced by depletion of γ-glutamylcyclotransferase. Biochemical and Biophysical Research Communications. 2018; 496: 218–224.

[36] Maheshwari M, Yadav N, Hasanain M, Pandey P, Sahai R, Choyal K, *et al*. Inhibition of p21 activates Akt kinase to trigger ROS-induced autophagy and impacts on tumor growth rate. Cell Death & Disease. 2022; 13: 1045.